Decision Analytics Journal 10 (2024) 100374

Contents lists available at ScienceDirect

Decision Analytics Journal

journal homepage: www.elsevier.com/locate/dajour

A deterministic model of COVID-19 with differential infectivity and vaccination booster

Stephane Y. Tchoumi [a,b,*,1], Elissa J. Schwartz [c,1], Jean M. Tchuenche [d,e,1]

[a] Department of Mathematics and Computer Sciences ENSAI, University of NGaoundéré, PO Box 455, Ngaoundéré, Cameroon
[b] Department of Mathematics and Applied Mathematics, University of Pretoria, South Africa
[c] Department of Mathematics & Statistics and School of Biological Sciences, Washington State University, PO Box 643113, Pullman, WA, 99164-3113, USA
[d] School of Computer Science and Applied Mathematics, University of the Witwatersrand, Johannesburg, South Africa
[e] School of Computational and Communication Sciences and Engineering, Nelson Mandela African Institution of Science and Technology, Arusha, Tanzania

ARTICLE INFO

Keywords:
Non-linear mathematical model
Simulation
COVID-19
Vaccination
Basic reproduction number
Sensitivity analysis

ABSTRACT

Vaccine boosters have been recommended to mitigate the spread of the coronavirus disease 2019 (COVID-19) pandemic. A mathematical model with three vaccine doses and susceptibility is formulated. The model is calibrated using the cumulative number of hospitalized cases from Alberta, Canada. Estimated values from the fitting are used to explore the potential impact of the booster doses to mitigate the spread of COVID-19. Sensitivity analysis on initial disease transmission shows that the most sensitive parameters are the contact rate, the vaccine efficacy, the proportion of exposed individuals moving into the symptomatic and asymptomatic classes, and the recovery rate from asymptomatic infection. Simulation results support the positive population-level impact of the second and third COVID-19 vaccine boosters to reduce the number of infections and hospitalizations. Public health policy and decision-makers should continue advocating and encouraging people to get booster doses. As the end of the pandemic is in sight, there should be no complacency before it resolves.

1. Introduction

Coronavirus disease 2019 (known as COVID-19) is an infectious disease caused by the severe acute respiratory syndrome coronavirus 2 (SARS-CoV-2) virus, first reported in the Hubei Province of China in December 2019. From this epicenter, COVID-19 spread all over the world. According to the World Health Organization (WHO), so far, there have been more than 771 million confirmed cases and close to 7 million deaths, with over 1.1 million deaths reported in the United States of America alone [1]. COVID-19 is transmitted by direct contact or by contact with infected surfaces. Several non-pharmaceutical measures have been implemented to curb the spread of the disease prior to the development of effective COVID-19 vaccines. These include social/physical distancing (staying at least 1 m apart from others), properly wearing a face mask, especially when in poorly ventilated settings, regular hand-washing with soap and water or use of alcohol-based hand sanitizer, covering the mouth and nose when coughing or sneezing, and isolation when unwell until recovery. Other stringent measures to suppress the spread of the virus were schools, shops, borders and workplace closure, and restriction of social gatherings [2,3]. These stringent measures have had negative economic repercussions for countries and people worldwide [4]. COVID-19 vaccination, however, has substantially altered the course of the pandemic [5].

Development of highly effective vaccines eventually proved important to curtail the spread of COVID-19 [6,7]. Within a short time period of one year, several pharmaceutical companies successfully developed various prototype vaccines against COVID-19. As of November 2022, the COVID-19 vaccine tracker showed that among 238 vaccine candidates, 49 have been approved for use in 201 countries, and 11 were granted emergency use by the WHO [8]. The majority of approved vaccines were messenger ribonucleic acid (mRNA) vaccines, which require two doses. The first dose introduces the targeted antigen into the body, while the second reinforces its action and prolongs the duration of the immune response, boosting the components of the immune system that provide broad antiviral protection [4,9].

By the end of August 2021, a booster with an mRNA vaccine against COVID-19 (3rd dose) was recommended for people over 65, those at high risk of severe diseases, and health care professionals, at least 6 months after the second dose. On September 17, 2021, the United States Food and Drug Administration's Advisory Committee on Vaccines and Related Biologicals issued a similar opinion on a marketing authorization extension application for the Pfizer-BioNTech vaccine (sold under the brand name Comirnaty) [10]. Administration of a third dose at least 6 months after the complete primary series strongly increases the neutralizing capacity of the serum, including against some of the most recent variants [10].

* Corresponding author at: Department of Mathematics and Computer Sciences ENSAI, University of NGaoundéré, PO Box 455, Ngaoundéré, Cameroon.
E-mail address: sytchoumi83@gmail.com (S.Y. Tchoumi).

[1] All authors contributed equally.

https://doi.org/10.1016/j.dajour.2023.100374
Received 20 July 2023; Received in revised form 10 November 2023; Accepted 28 November 2023
Available online 2 December 2023

Since the introduction of COVID-19 vaccination, several mathematical modeling studies have investigated the impact of a single dose vaccine on the dynamics of COVID-19 [4,11–17]. Anip et *al.*, [18] proposed a COVID-19 model with a double-dose vaccination strategy to control the outbreak in Bangladesh. They noted that a full dose vaccination program significantly reduces the mild and critical cases and has the potential to eradicate the virus from the community. However, they assumed that the effectiveness of the vaccine is 100%, that is to say a vaccinated person cannot become infected, which given what we know about the epidemiology of COVID-19, is not very realistic. Also, they neither included waning of the vaccine after the second dose, nor the waning natural immunity. A model predictive control approach to optimally devise a two-dose vaccination roll out was investigated in [19]. Dosing interval strategies and optimizing COVID-19 vaccination programs during vaccine shortages have been respectively studied in [4,20]. While the common strategies typically rely on the prioritization of the different classes of individuals, Scarabaggio et al., [21] proposed a model predictive approach to optimally control multi-dose vaccine administration when the available number of doses is not sufficient for the entire population. Focusing on the minimization of the expected number of deaths, their approach discriminates between the number of first and second doses, thus considering also the possibility that some individuals may receive only one vaccine dose if the resulting expected fatalities are low. Reyes et al., [22] highlighted the importance of attaining full (two-dose) vaccination status, that is, completing vaccination schedules to reduce the adverse outcomes during the pandemic. Wang et al. [23] investigated a deterministic model with two vaccine doses (partially vaccinated with 1 dose and individuals who received their second dose), but no booster.

We formulate a model taking into account three doses of vaccination, as well as differential susceptibility, and investigate the impact of the booster dose of vaccination on mitigating the spread of COVID-19. Thus, our proposed model aims to address the impact of three doses (two doses plus one booster) of the vaccine on the transmission dynamics of the disease, where each subsequent dose makes a person incrementally less likely to move from the uninfected class to the exposed class. Each subsequent dose also affects vaccine waning and the waning of natural immunity (that is, movement from the recovered class back to the susceptible class), and in addition, the model incorporates infections from asymptomatic individuals. We also investigate the additional benefits, in terms of preventing hospitalizations, deaths, and symptomatic infections, with each subsequent booster dose of the COVID-19 vaccine.

This paper is organized as follows. The proposed mathematical model is formulated in Section 2. Standard analyses of the model such as well-posedness, positivity and boundedness of solutions, derivation of the basic reproduction number, stability of the model equilibria, and the existence of possible positive solutions are carried out in Section 3. Numerical simulations are provided in Section 4, where the model is fitted using data from Alberta, Canada. The paper ends with a discussion of the implications of model results in Section 5.

2. Model formulation

Based on the epidemiological status of individuals and the clinical progression of COVID-19, the total population $N(t)$ is stratified into twelve compartments according to individuals' COVID-19 status: susceptible individuals (S), individuals vaccinated with one dose of vaccine (V_1), individuals vaccinated with two doses of vaccine (V_2), individuals vaccinated with three doses of vaccine (V_3), exposed individuals (E_1) and (E_2), asymptomatic (I_1^a) and (I_2^a), symptomatic (I_1^s) and (I_2^s), hospitalized (H), and recovered individuals (R). For all $t \geq 0$,

$$N(t) = S(t) + V_1(t) + V_2(t) + V_3(t) + E_1(t) + E_2(t) + I_1^a(t) + I_1^s(t) + I_2^a(t) + I_2^s(t) + H(t) + R(t).$$

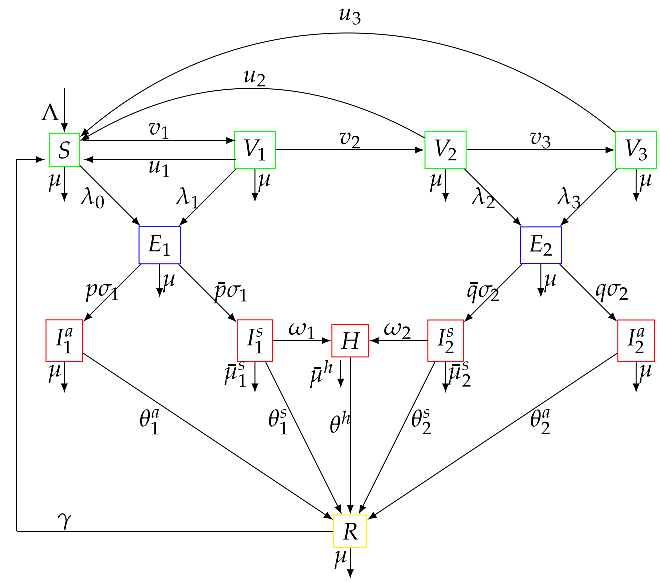

Fig. 1. Flow diagram of the model where for simplicity, $\bar{p} = 1-p$, $\bar{q} = 1-q$, $\bar{\mu}_1^s = \mu + \mu_1^s$, $\bar{\mu}_2^s = \mu + \mu_2^s$ and $\bar{\mu}^h = \mu + \mu^h$.

The population is recruited at a constant rate Λ, and dies naturally at rate μ. In addition to this natural death, symptomatic infectious I_1^s, I_2^s and hospitalized H die due to the disease at the respective COVID-19-induced death rates μ_1^s, μ_2^s, and μ^h.

Susceptible individuals are vaccinated with the first vaccine dose at the rate v_1. Following a second dose, they move into the class of vaccinated with two doses V_2 at the rate v_2, and at the rate v_3 they become vaccinated with the third dose V_3. Due to vaccine waning, the individuals of classes V_1, V_2 and V_3 lose their immunity at the respective rates u_1, u_2 and u_3 to become susceptible.

Because the vaccine is imperfect, vaccinated individuals may still be differentially susceptible to the infection [24–28], which may lead to the emergence of variants [29]. Such leaky vaccine also provide imperfect but widespread protection to the masses [30–32], but infection-blocking efficacy is always beneficial in reducing disease spread within the community [33]. Thus, a susceptible individual or vaccinated individuals with one, two or three doses who comes in contact with an infected individual can become infected, with a force of infection

$$\lambda_i = \beta(1-\epsilon_i)\frac{I_1^s + I_2^s + H + \xi_1 I_1^a + \xi_2 I_2^a}{N}, \quad i = 0, \dots, 3.$$

After the latency period, exposed individuals with zero or one dose of vaccine in E_1 become infectious at the rate σ_1, with the probability p of being asymptomatic I_1^a, and $1-p$ of being symptomatic I_1^s, while those in E_2 become infectious at the rate σ_2, with probability q of being asymptomatic I_2^a, and $1-q$ of being symptomatic I_2^s. Symptomatic infectious individuals I_1^s and I_2^s become hospitalized at the respective rates ω_1 and ω_2.

All infectious individuals in I_1^a, I_2^a, I_1^s, I_2^s and H recover at the respective rates θ_1^a, θ_2^a, θ_1^s, θ_2^s and θ^h and move to the recovered class R. The loss of natural immunity occurs at the rate γ, and recovered individuals move back to the susceptible class S.

The description of all the states variables and model parameters are summarized respectively in Tables 1 and 2. We note that $\epsilon_0 = 0$ and assume that for $i = 1, \dots, 3, 0$, the model parameters satisfy the following $0 \leq \epsilon_i < 1$, $0 < p, q < 1$, $\xi_1 > \xi_2$, $\epsilon_1 < \epsilon_2 < \epsilon_3$, $v_1 > v_2 > v_3$, $\sigma_1 > \sigma_2$, $\omega_1 > \omega_2$, $\mu < \mu_2^s < \mu_1^s < \mu^h$, and $\theta_2^a > \theta_1^a > \theta_2^s > \theta_1^s > \theta^h$.

From the model flowchart of COVID-19 transmission dynamics depicted in Fig. 1, we derive the following non-linear system of ordinary

Table 1
State variables and their descriptions.

Variables	Description
S	Susceptible individuals
V_1	Individuals vaccinated with one dose of vaccine
V_2	Individuals vaccinated with two doses of vaccine
V_3	Individuals vaccinated with three doses of vaccine
E_1	Exposed individuals after zero or one dose of vaccine
E_2	Exposed individuals after two or three doses of vaccine
I_1^a	Asymptomatic infected individuals with zero or one dose of vaccine
I_2^a	Asymptomatic infected individuals with two or three doses of vaccine
I_1^s	Symptomatic infected individuals with zero or one dose of vaccine
I_2^s	Symptomatic infected individuals with two or three doses of vaccine
H	Hospitalized individuals
R	Recovered individuals

Table 2
Model parameters.

Parameters	Description	Value	Reference
Λ	Recruitment rate	1000	
v_i	Rate of ith vaccination	Fitted	
u_i	Vaccine waning after the ith dose	Fitted	
β	Transmission rate	Fitted	
σ_1	Progression rate from E_1 to I_1^a with probability p and to I_1^s with probability $1-p$	0.12	
σ_2	Progression rate from E_2 to I_2^a with probability q and to I_2^s with probability $1-q$	0.12	
θ_1^a	Recovery rate of I_1^a	$\frac{1}{19}$	Assumed
θ_1^s	Recovery rate of I_1^s	$\frac{1}{20}$	Assumed
θ_2^a	Recovery rate of I_2^a	$\frac{1}{18}$	Assumed
θ_2^s	Recovery rate of I_2^s	$\frac{1}{21}$	[18]
θ^h	Recovery rate of H	Fitted	
γ	Waning immunity rate	0.11	
ω_1	Hospitalization rate of I_1^s	0.87	[18]
ω_2	Hospitalization rate of I_2^s	0.57	Assumed
ε_i	Vaccine efficacy after the i^{th} vaccination	Fitted	
ξ_1	Fraction of infectiousness due to asymptomatic infection in unvaccinated or single-vaccinated individuals	0.05	
ξ_2	Fraction of infectiousness due to asymptomatic infection in double or triple-vaccinated individuals	0.01	
μ	Natural death rate	$\frac{1}{70\times 365}$	[34]
μ^h	Death rate due to symptomatic infection in hospitalized individuals	0.009	
μ_1^s	Death rate due to symptomatic infection in unvaccinated or single-vaccinated individuals	0.009	
μ_2^s	Death rate due to symptomatic infection in double or triple-vaccinated individuals	0.009	

differential equations:

$$
\begin{aligned}
\dot{S} &= \Lambda + \gamma R + u_1 V_1 + u_2 V_2 + u_3 V_3 - (\lambda_0 + v_1 + \mu) S,\\
\dot{V}_1 &= v_1 S - (\lambda_1 + u_1 + v_2 + \mu) V_1,\\
\dot{V}_2 &= v_2 V_1 - (\lambda_2 + u_2 + v_3 + \mu) V_2,\\
\dot{V}_3 &= v_3 V_2 - (\lambda_3 + u_3 + \mu) V_3,\\
\dot{E}_1 &= \lambda_0 S + \lambda_1 V_1 - (\sigma_1 + \mu) E_1,\\
\dot{E}_2 &= \lambda_2 V_2 + \lambda_3 V_3 - (\sigma_2 + \mu) E_2,\\
\dot{I}_1^a &= p\sigma_1 E_1 - (\theta_1^a + \mu) I_1^a,\\
\dot{I}_1^s &= (1-p)\sigma_1 E_1 - (\theta_1^s + \omega_1 + \mu + \mu_1^s) I_1^s,\\
\dot{I}_2^a &= q\sigma_2 E_2 - (\theta_2^a + \mu) I_2^a,\\
\dot{I}_2^s &= (1-q)\sigma_2 E_2 - (\theta_2^s + \omega_2 + \mu + \mu_2^s) I_2^s,\\
\dot{H} &= \omega_1 I_1^s + \omega_2 I_2^s - (\theta^h + \mu + \mu^h) H,\\
\dot{R} &= \theta_1^a I_1^a + \theta_1^s I_1^s + \theta_2^a I_2^a + \theta_2^s I_2^s + \theta^h H - (\gamma + \mu) R,
\end{aligned} \tag{1}
$$

with initial conditions

$$
\begin{aligned}
&S(0) > 0,\ V_1(0) \ge 0,\ V_2(0) \ge 0,\ \ V_3(0) \ge 0,\\
&E_1(0) \ge 0,\ E_2(0) \ge 0,\ I_1^a(0) \ge 0,\ \ I_1^s(0) \ge 0,\\
&I_2^a(0) \ge 0,\ I_2^s(0) \ge 0,\ H(0) \ge 0,\ \ R(0) \ge 0.
\end{aligned} \tag{2}
$$

The force of infection if given by

$$\lambda_i = \beta\left(1-\varepsilon_i\right) \frac{I_1^s + I_2^s + H + \xi_1 I_1^a + \xi_2 I_2^a}{N}, \quad \text{with} \quad i = 0, \dots, 3.$$

The parameters, their description, values and sources are provided in Table 2.

3. Model analysis

Since the model system (1) with initial conditions (2) monitors human populations, all associated state variables and parameters are non-negative for all time $t \ge 0$. By adding all the equations in the model system (1), and solving the resulting differential inequality (by applying Gronwall's Lemma) yields $N(t) \le \dfrac{\Lambda}{\mu}$, $\forall t > 0$. The region

$$\Omega = \left\{ \left(S, V_1, V_2, V_3, E_1, E_2, I_1^a, I_1^s, I_2^a, I_2^s, H, R\right) \in \mathbb{R}_+^{12} : N \le \frac{\Lambda}{\mu} \right\}$$

is positively-invariant and attracting as it can be shown that all solutions of the model system (1) starting in Ω remain in Ω for all $t \ge 0$.

3.1. Disease-free equilibrium and basic reproduction number

Let

$$
\begin{aligned}
&g_1 = \sigma_1 + \mu,\ g_2 = \sigma_2 + \mu,\ g_3 = \theta_1^a + \mu,\ g_4 = \theta_1^s + \omega_1 + \mu + \mu_1^s,\\
&\quad g_5 = \theta_2^a + \mu,\ g_6 = \theta_2^s + \omega_2 + \mu + \mu_2^s,\ g_7 = \theta^h + \mu + \mu^h,
\end{aligned}
$$

$$G_1 = v_1 + \mu,\ G_2 = u_1 + v_2 + \mu,\ G_3 = u_2 + v_3 + \mu,\ G_4 = u_3 + \mu.$$

The model system (1) has a disease-free equilibrium (DFE) given by

$$\mathcal{E}_0 = (X_S^0, X_I^0) = (X_S^0, 0) = \left(S^0, V_1^0, V_2^0, V_3^0, 0, 0, 0, 0, 0, 0, 0, 0\right),$$

where

$$\begin{aligned} S^0 &= \frac{\Lambda G_2 G_3 G_4}{\left(v_1 v_2 v_3 + \left(\left(\mu + u_1 + v_1 + v_2\right)\left(\mu + u_2 + v_3\right) + v_1 v_2\right)\left(\mu + u_3\right)\right)\mu}, \\ V_1^0 &= \frac{v_1}{G_2} S^0, \\ V_2^0 &= \frac{v_1 v_2}{G_2 G_3} S^0, \\ V_3^0 &= \frac{v_1 v_2 v_3}{G_2 G_3 G_4} S^0. \end{aligned} \tag{3}$$

Using the next-generation method [35,36], the effective reproduction number $\mathcal{R}_c(v_1, v_2, v_3)$ and the basic reproduction number $\mathcal{R}_0$ are given respectively by

$$\mathcal{R}_c(v_1, v_2, v_3) = \mathcal{R}_1 + \mathcal{R}_2, \tag{4}$$

where

$$\mathcal{R}_1 = \frac{\mu g_2 g_5 g_6 \sigma_1 \left(\beta S^0 + \beta_1 V_1^0\right)\left[g_4 g_7 p \xi_1 + g_3 (1-p)(g_7 + \omega_1)\right]}{g_1 g_2 g_3 g_4 g_5 g_6 g_7 \Lambda},$$

$$\mathcal{R}_2 = \frac{\mu g_1 g_3 g_4 \sigma_2 \left(\beta_2 V_2^0 + \beta_3 V_3^0\right)\left[g_6 g_7 q \xi_2 + g_5 (1-q)(g_7 + \omega_2)\right]}{g_1 g_2 g_3 g_4 g_5 g_6 g_7 \Lambda},$$

and

$$\mathcal{R}_0 = \mathcal{R}_c(0,0,0) = \frac{\sigma_1 \beta \left[g_4 g_7 p \xi_1 + g_3 (1-p)(g_7 + \omega_1)\right]}{g_1 g_3 g_4 g_7}. \tag{5}$$

Proof. The proof is provided in Appendix A. ■

Remark 1. The effective reproduction number $\mathcal{R}_c(v_1, v_2, v_3)$ is defined as the average number of secondary infections generated by a single infectious individual during the entire duration of infectiousness in a totally susceptible population when vaccination is implemented. [25].

3.2. Global stability of the DFE

To prove the global asymptotic stability (GAS) of the DFE, we use the approach in [37]. We first re-write the COVID-19 model (1) as follows:

$$\begin{cases} \dfrac{dX}{dt} &= F(X, I), \\ \dfrac{dI}{dt} &= \mathcal{G}(X, I), \quad \mathcal{G}(X, 0) = 0, \end{cases} \tag{6}$$

in which $X = \left(S, V_1, V_2, V_3, R\right) \in \mathbb{R}^5$ and $I = \left(E_1, E_2, I_1^a, I_1^s, I_2^a, I_2^s, H\right) \in \mathbb{R}^7$. We note here that X and I represents the classes of the uninfectious and infectious individuals respectively. For our model to be GAS at $\mathcal{E}_0$, it needs to satisfy the following conditions as adopted from [37], which are

($\mathcal{C}_1$) Local stability is guaranteed at $\mathcal{E}_0$ whenever $\mathcal{R}_c(v_1, v_2, v_3) < 1$.
($\mathcal{C}_1$) At $\dfrac{dX}{dt} = F(X_0, 0)$, the DFE is globally asymptotically stable.
($\mathcal{C}_3$) $\mathcal{G}(X, I) = \mathcal{A} I - \hat{\mathcal{G}}(X, I)$, $\hat{\mathcal{G}}(X, I) \geq 0$ for $(X, I) \in \Omega$, where $\mathcal{A} = \mathcal{D}_I \mathcal{G}(\mathcal{E}_0)$ is a Metzler matrix and Ω is the biologically feasible region defined earlier.

Theorem 2. *If the disease-induced death rates are zero, that is ($\mu_s^1 = \mu_s^2 = \mu^h = 0$) and $N(0) \in \Omega$, then, the disease-free equilibrium $\mathcal{E}_0$ is globally asymptotically stable (GAS) when $\mathcal{R}_c(v_1, v_2, v_3) < 1$.*

Proof. A detailed proof is provided in Appendix B. ■

3.3. Endemic equilibrium

For mathematical tractability and convenience, assume that there is no waning immunity, that is, $u_2 = u_3 = 0$, and $\gamma = 0$. The endemic equilibrium $\mathcal{E}_1 = (S^\star, V_1^\star, V_2^\star, V_3^\star, E_1^\star, E_2^\star, I_1^{a\star}, I_1^{s\star}, I_2^{a\star}, I_2^{s\star}, H^\star, R^\star)$ is given by the solution of the following system:

$$\begin{aligned} &\Lambda + u_1 V_1^\star - (\lambda_0 + G_1) S^\star = 0, \\ &v_1 S^\star - (\lambda_1 + G_2) V_1^\star = 0, \\ &v_2 V_1^\star - (\lambda_2 + G_3) V_2^\star = 0, \\ &v_3 V_2^\star - (\lambda_3 + G_4) V_3^\star = 0, \\ &\lambda_0 S^\star + \lambda_1 V_1^\star - g_1 E_1^\star = 0, \\ &\lambda_2 V_2^\star + \lambda_3 V_3^\star - g_2 E_2^\star = 0, \\ &p \sigma_1 E_1^\star - g_3 I_1^{a\star} = 0, \\ &(1-p) \sigma_1 E_1^\star - g_4 I_1^{s\star} = 0, \\ &q \sigma_2 E_2^\star - g_5 I_2^{a\star} = 0, \\ &(1-q) \sigma_2 E_2^\star - g_6 I_2^{s\star} = 0, \\ &\omega_1 I_1^{s\star} + \omega_2 I_2^{s\star} - g_7 H^\star = 0, \\ &\theta_1^a I_1^{a\star} + \theta_1^s I_1^{s\star} + \theta_1^h H^\star + \theta_2^a I_2^{a\star} + \theta_2^s I_2^{s\star} - G_5 R^\star = 0. \end{aligned} \tag{7}$$

The number of positive solutions of the system (7) depends on the value of $\mathcal{R}_c$. The following result summarizes the different possible cases.

Theorem 3. *The model (1) admits*

- *0, 2 or 4 endemic equilibria if $\mathcal{R}_c < 1$,*
- *0, 1, 2 or 3 endemic equilibria if $\mathcal{R}_c = 1$,*
- *1 or 3 endemic equilibria if $\mathcal{R}_c > 1$.*

Proof. See Appendix C for the proof. ■

4. Numerical simulations

Numerical simulations of the model system (1) are carried out, using the parameter values given in Table 2. Since the model takes into account a lot of the actual variability reported among individuals affected with COVID-19, it offers an opportunity to evaluate these differences. First, using data on the cumulative number of COVID-19 hospitalized individuals from Alberta, Canada [38], we fitted the model to estimate COVID-19 parameter values for vaccine efficacy, vaccination rate, vaccine waning, the recovery rate from hospitalized infected individuals, and the transmission rate. Next, we used our parameterized model to numerically investigate the effect of different probabilities of developing asymptomatic or symptomatic infection on the following outcomes: hospitalization; the numbers of symptomatic infections among those with zero or one vaccine dose, or those with two or three vaccine doses; and the numbers of asymptomatic infections among those with zero or one vaccine dose, or those with two or three vaccine doses. We also simulated the impact of a booster dose (i.e., the third dose) of COVID-19 vaccination on reducing hospitalizations, symptomatic infections, and asymptomatic infections in Alberta, and evaluated the effect of waning of the booster dose on symptomatic and asymptomatic infections. Finally, we conducted a sensitivity analysis using Latin Hypercube Sampling and Partial Rank Correlation Coefficients on initial disease transmission.

4.1. Parameter estimation

The model was fitted to data on the cumulative hospitalized cases in Alberta, Canada [38], for a period of 100 days starting March 6, 2020. The fitting was performed in Python using the minimize function. The fitted parameters are $\beta = 0.7983$, $\theta^h = 0.001$, $v_1 = 0.6163$, $v_2 = 0.5327$, $v_3 = 0.1988$, $u_1 = 0.8896$, $u_2 = 0.5620$, $u_3 = 3.2485 \times 10^{-8}$, $\epsilon_1 =$

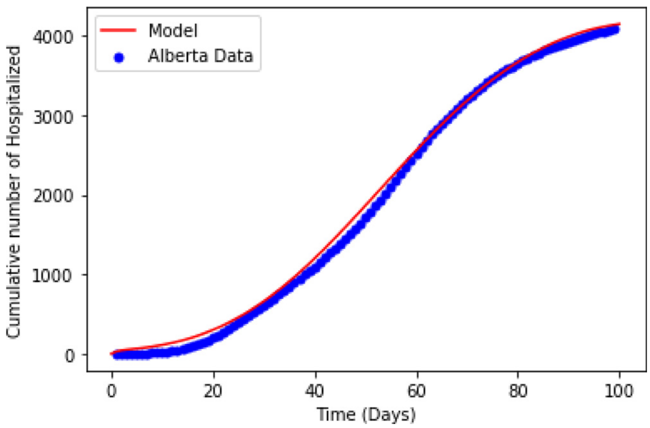

Fig. 2. Fitting of the cumulative number of hospitalized COVID-19 cases in Alberta.

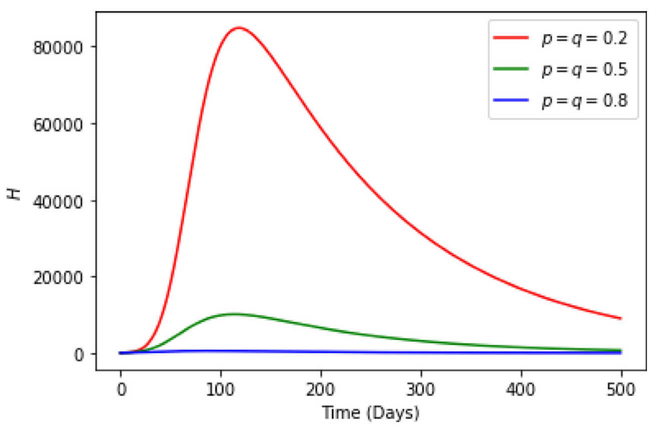

Fig. 3. Evolution of numbers of hospitalized in Alberta.

0.2816, $\varepsilon_2 = 0.0294$, $\varepsilon_3 = 0.89$. With these estimated parameters, the data for Alberta fits the model very well, as shown in Fig. 2.

4.2. Effects of the probabilities p of progression from E_1 to I_1^a, and q of moving from E_2 to I_2^a

We next investigated the effect on epidemic dynamics of the probability of asymptomatic or symptomatic infection, by simulating model trajectories over 500 days. Variation in the probability of an infection being symptomatic or asymptomatic played an interesting role in our model dynamics. In terms of hospitalizations, the model predicted that the greatest number of hospitalized cases occurred when the probability of asymptomatic infection was smallest (p, q low), and hospitalization was lowest when the probability of asymptomatic infection was highest (p, q high), as seen in Fig. 3. In fact, when $p = q = 0.8$, hospitalization was near zero in Alberta. Hospitalizations were minimal (in terms of magnitude of the peak) when $p = q = 0.5$ (i.e., an equal chance of an infected individual becoming symptomatic or asymptomatic). Equivalent trends were seen in symptomatic infections (either among those with zero or one vaccination, or among those with two or three vaccinations), as seen in Figs. 4 and 5, except that the numbers declined more rapidly after peak infection as compared to hospitalizations. Similar trends were found with asymptomatic cases (again, either among those with zero or one vaccination, or among those with two or three vaccinations) as shown in Figs. 6 and 7, in that infections were greater with small probabilities (p, q low), except that the number of asymptomatic infections when $p = 0.8$ or $q = 0.8$ was not negligible,

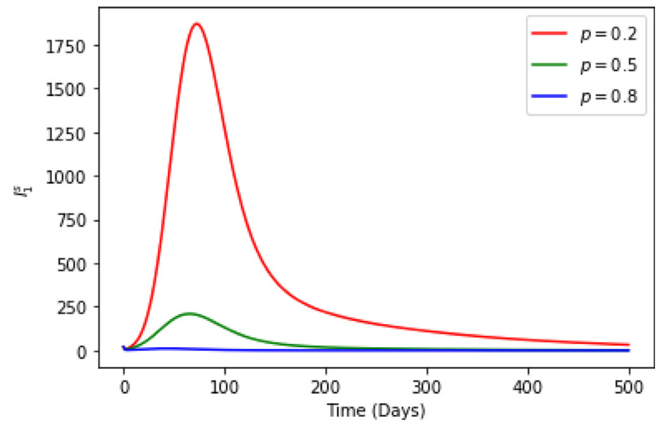

Fig. 4. Evolution of numbers of symptomatic I_1^s in Alberta.

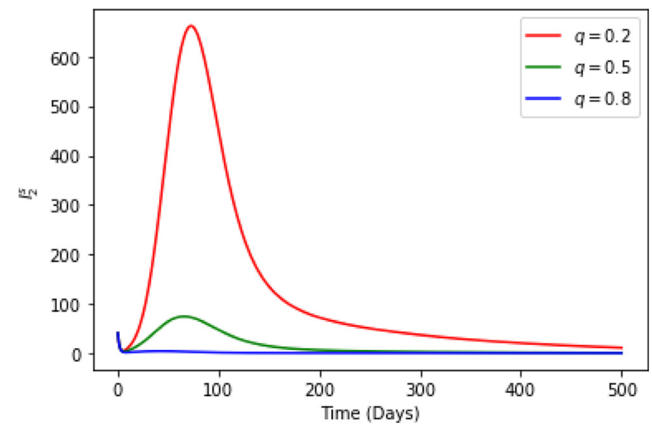

Fig. 5. Evolution of numbers of symptomatic I_2^s in Alberta.

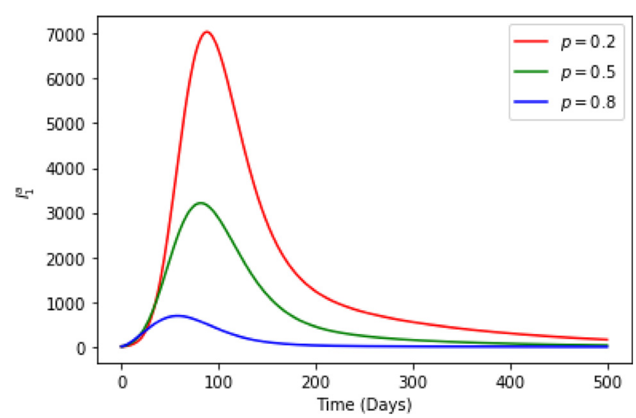

Fig. 6. Evolution of numbers of asymptomatic I_1^a in Alberta.

and asymptomatic cases were predicted to be intermediate when $p = q = 0.5$.

4.3. Effects of booster vaccination rate

Model simulations showed that a hundredfold increase in the booster dose vaccination rate gave a substantial reduction in the hospitalization rate (Fig. 8). Interestingly, a tenfold increase in boosters only minimally reduced the peak in hospitalized infections. Similar results were found with the number of symptomatic infections, as well as asymptomatic

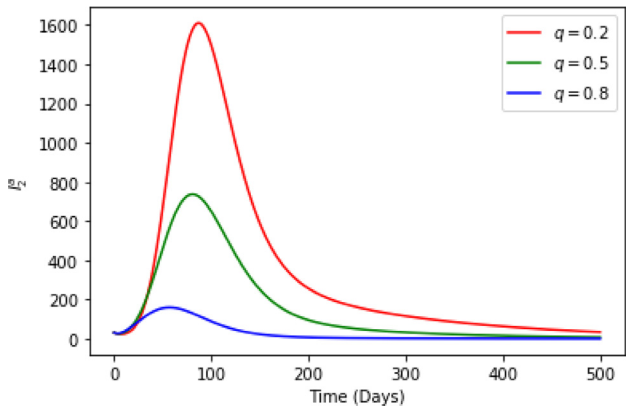

Fig. 7. Evolution of numbers of asymptomatic I_2^a in Alberta.

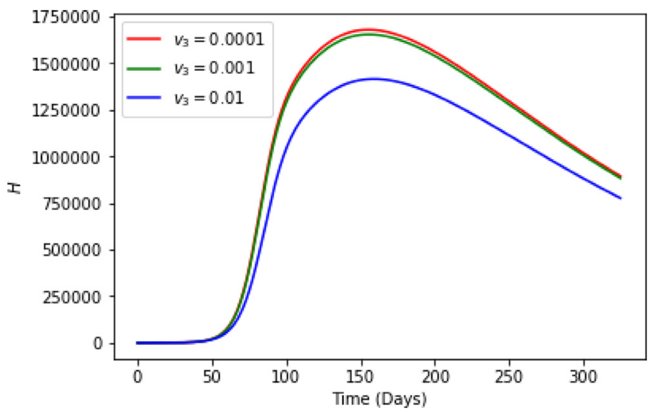

Fig. 8. Evolution of numbers of hospitalized in Alberta.

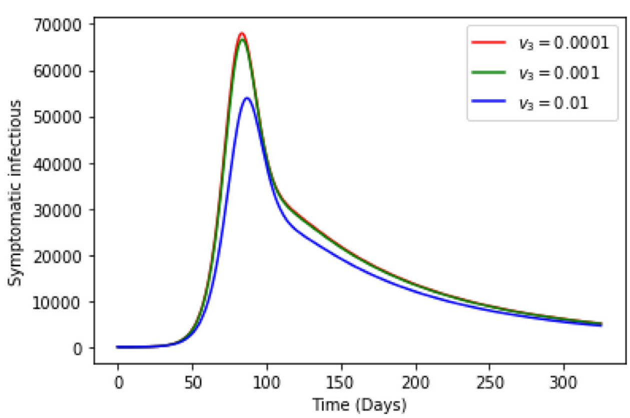

Fig. 9. Evolution of numbers of symptomatic in Alberta.

infections. Specifically, a tenfold increase in the rate of booster vaccinations decreased the symptomatic infections only marginally, but a hundredfold increase in boosters greatly reduced symptomatic infections (Fig. 9). Likewise, increasing the rate of vaccination with the booster one hundredfold substantially reduced asymptomatic infections (Fig. 10), while modest reductions were seen in symptomatic infections with a tenfold reduction in booster vaccination.

4.4. Effects of waning of booster

When the waning of the booster vaccination is varied, shortening the waning rate (i.e., lengthening the duration of the booster vaccine's

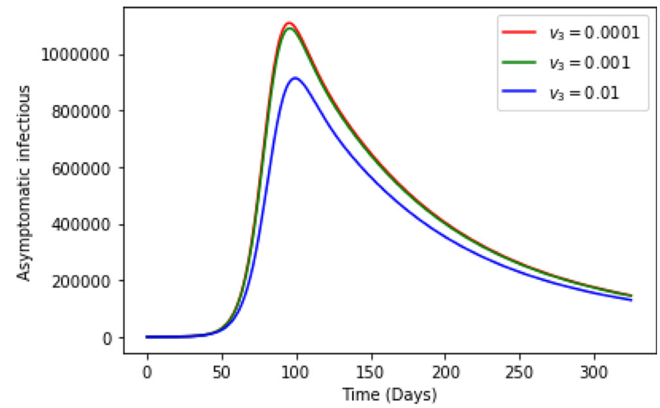

Fig. 10. Evolution of numbers of asymptomatic in Alberta.

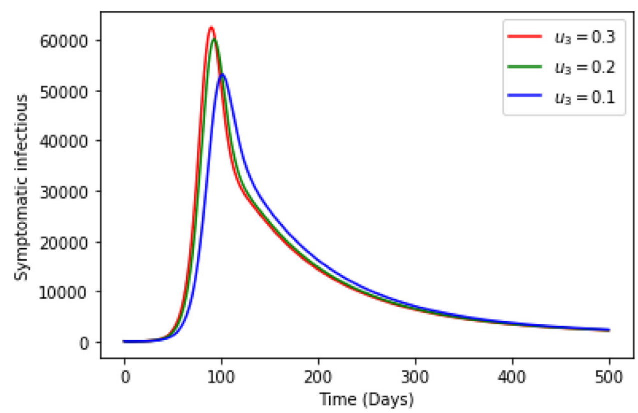

Fig. 11. Evolution of numbers of symptomatic in Alberta.

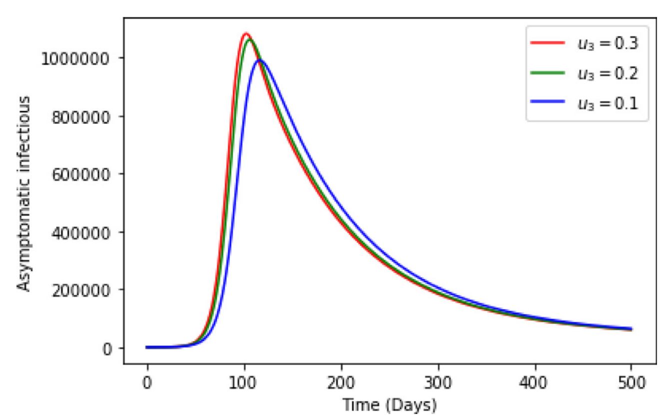

Fig. 12. Evolution of numbers of asymptomatic in Alberta.

effectiveness) resulted in a lower number of symptomatic infections (Fig. 11), as well as asymptomatic infections (Fig. 12). Our simulations also showed that a booster vaccine that wanes more slowly delays the peak of infection (Figs. 11 and 12).

4.5. Sensitivity analysis and PRCCs on initial disease transmission

Mathematical models, being symbolic representations of real life systems, by construction they inherit the loss of information which

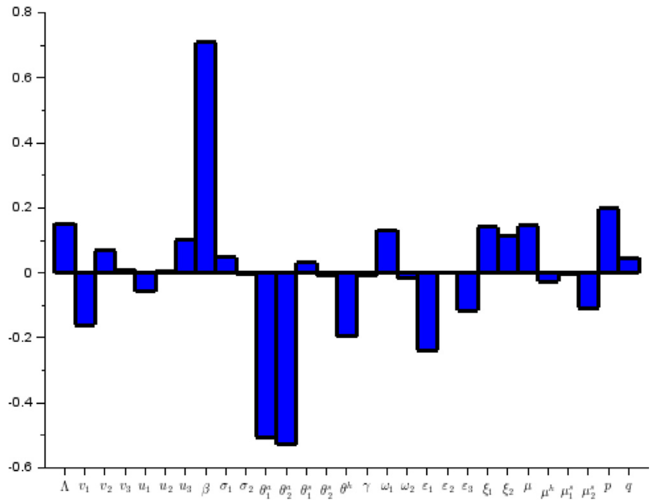

Fig. 13. PRCCs showing the effect of varying the model input parameters on $\mathcal{R}_c$.

could make the prediction of model outcomes imprecise [39]. Sensitivity analyses could help determine key model parameters that have the highest effect on the disease to guide policy and health decision makers on which parameter to prioritize and consequently which intervention(s) to implement [40] . Using Partial Rank Correlation Coefficients and Latin Hypercube Sampling, sensitivity analysis is carried out to determine the relative importance of model parameters to initial disease transmission. Fig. 13 depicts the sensitivity indices of the effective reproduction number $\mathcal{R}_c$. Parameters with a sensitivity index greater than 0.5 in absolute value are the most sensitive, and modifying them can influence the value of the effective reproduction number $\mathcal{R}_c$, and thereby the behavior of the disease transmission dynamics. The most sensitive parameters are the transmission/contact rate β and the recovery rates from asymptomatic infections θ_1^a and θ_2^a. Negative indices mean that the increase in the relevant parameters leads to the decrease in the disease reproductive number. Thus, intervention measures should target increasing the parameters with negative indices and decreasing those with positive indices.

5. Conclusion

The COVID-19 pandemic has been a global public health challenge as the disease caused substantial morbidity and mortality worldwide from its emergence in 2020. We formulated and analyzed a deterministic model of COVID-19 taking into account three doses of vaccination to investigate the potential impact of the highly recommended COVID-19 booster vaccine dose to mitigating the spread of the disease. The model is then calibrated using the cumulative number of hospitalized cases from Alberta, Canada.

Results showed that mathematical modeling of booster vaccination and differential infectivity uncovered insights that were not previously obvious. For our data set, hospitalizations and symptomatic infections could be nearly brought to zero if 80% of infections are without symptoms (i.e., $p = q = 0.8$). Alternatively, if the chance of asymptomatic infection is low, then both asymptomatic and symptomatic infections are high. An increase in the rate of booster vaccination (e.g., by a hundredfold) reduces hospitalizations, symptomatic cases, and asymptomatic cases; however, a marginal increase (e.g., tenfold) in the booster vaccination rate does not necessarily show a noticeable difference. Interestingly, the model simulations showed that variation in vaccine waning rates affect not only the magnitude of the infection peak but also the timing of the peak. In boosters with longer lasting duration (i.e., boosters with lower waning rates), the peak of infection is reduced as well as delayed.

The sensitivity analysis identified the key parameters behind initial disease transmission. These include the contact/transmission rate (which is positively correlated), recovery from asymptomatic infection among those with two or three vaccine doses (which is negatively correlated), and recovery from asymptomatic infection among those with zero or one vaccine dose (which is negatively correlated). A more minor role is played by the fraction of infectiousness due to asymptomatic infection in those with two or three vaccine doses (which is positively correlated). The impacts can be clearly understood due to the observation that β and ξ are in the numerator of the force of infection, so increasing them will increase the disease reproduction number; in other words, it can be seen that increasing contact or virus transmission, and increasing the contribution to transmission of asymptomatic infection even in double or triply vaccinated individuals, will increase infection. In the opposite direction, the recovery of asymptomatic infected individuals with two or three vaccine doses reduces the number of infected individuals by moving them into the immune class, so increasing this rate will decrease the disease reproductive number, thereby decreasing infection. The implications of these results are that interventions to control infection include reducing contact/transmission, increasing recovery (specifically among doubly and triply vaccinated individuals with asymptomatic infection) and decreasing the fraction of infectiousness among asymptomatic (particularly among doubly and triply vaccinated individuals). In summary,

- If 80% of infected individuals are asymptomatic, hospitalizations and symptomatic infections could greatly be minimized.
- Booster vaccination rate increase reduces hospitalizations, symptomatic cases, and asymptomatic cases.
- Variation in vaccine waning rates affect not only the magnitude of the infection peak but also the timing of the peak.
- Transmission of asymptomatic infections even in doubly or triply vaccinated individuals could increase COVID-19 infections.
- Key COVID-19 intervention measures should target reducing contact/transmission, increasing treatment and vaccine booster rate.
- Health policy and decision-makers should continue advocating and encouraging people to get booster doses.

The proposed model is not exhaustive and can be extended in several ways. A fourth COVID-19 vaccine dose has been recommended to fight against the most recent Omicron variant and one could extend the model to include a fourth vaccination class. Also, we assumed that vaccines wear off to the S class only. Waning to the most recent class could provide some additional insights into the disease dynamics. While mathematical tractability could preclude standard analysis from a more complex model, numerical simulations could provide a pathway around a daunting theoretical analysis. Finally, a bifurcation analysis (that is the investigation of the co-existence of both a stable disease-free and endemic equilibria) could offer valuable additional insights into the model's dynamics.

Declaration of competing interest

All authors declare no potential conflict of interest.

Data availability

Data will be made available on request.

Acknowledgments

We would like to thank Stacey R. Smith? for helpful suggestions. SYT acknowledges the financial support from the DST/NRF SARChI Chair in Mathematical Models and Methods in Biosciences and Bioengineering at the University of Pretoria, grant No. 82770. Thanks to the reviewers for their comments and suggestions to enhance the manuscript.

$$F = \begin{pmatrix} 0 & 0 & \xi_1\dfrac{\beta S^0+\beta_1 V_1^0}{N^0} & \dfrac{\beta S^0+\beta_1 V_1^0}{N^0} & \xi_2\dfrac{\beta S^0+\beta_1 V_1^0}{N^0} & \dfrac{\beta S^0+\beta_1 V_1^0}{N^0} & \dfrac{\beta S^0+\beta_1 V_1^0}{N^0} \\ 0 & 0 & \xi_1\dfrac{\beta_2 V_2^0+\beta_3 V_3^0}{N^0} & \dfrac{\beta_2 V_2^0+\beta_3 V_3^0}{N^0} & \xi_2\dfrac{\beta_2 V_2^0+\beta_3 V_3^0}{N^0} & \dfrac{\beta_2 V_2^0+\beta_3 V_3^0}{N^0} & \dfrac{\beta_2 V_2^0+\beta_3 V_3^0}{N^0} \\ 0&0&0&0&0&0&0 \\ 0&0&0&0&0&0&0 \\ 0&0&0&0&0&0&0 \\ 0&0&0&0&0&0&0 \\ 0&0&0&0&0&0&0 \end{pmatrix}, \quad (12)$$

Box I.

Appendix A. Derivation of the reproduction number

The disease free equilibrium is the solution $\mathcal{E}^0 = (S^0, V_1^0, V_2^0, V_3^0, 0, 0, 0, 0, 0, 0, 0, 0)$ of the following system

$$\begin{array}{lcl} \Lambda + u_1 V_1^0 + u_2 V_2^0 + u_3 V_3^0 - (v_1+\mu)S^0 & = & 0, \\ v_1 S^0 - (u_1+v_2+\mu)V_1^0 & = & 0, \\ v_2 V_1^0 - (u_2+v_3+\mu)V_2^0 & = & 0, \\ v_3 V_2^0 - (u_3+\mu)V_3^0 & = & 0. \end{array} \quad (8)$$

Let $G_1 = v_1+\mu,\ G_2 = u_1+v_2+\mu,\ G_3 = u_2+v_3+\mu,\ G_4 = u_3+\mu$.

After some algebraic computations, we obtain

$$\begin{array}{lcl} S^0 & = & \dfrac{\Lambda G_2 G_3 G_4}{\left(v_1 v_2 v_3 + \left((\mu+u_1+v_1+v_2)(\mu+u_2+v_3)+v_1 v_2\right)(\mu+u_3)\right)\mu}, \\ V_1^0 & = & \dfrac{v_1}{G_2} S^0, \\ V_2^0 & = & \dfrac{v_1 v_2}{G_2 G_3} S^0, \\ V_3^0 & = & \dfrac{v_1 v_2 v_3}{G_2 G_3 G_4} S^0. \end{array} \quad (9)$$

Using the next-generation method [35,36], the rate of appearance of new infections $\mathcal{F}$ and the rate of transfer of individuals by all other means $\mathcal{V}$ are given by the following at least twice continuously differentiable functions

$$\mathcal{F} = \begin{pmatrix} \lambda_0 S + \lambda_1 V_1 \\ \lambda_2 V_2 + \lambda_3 V_3 \\ 0 \\ 0 \\ 0 \\ 0 \\ 0 \end{pmatrix}, \quad (10)$$

$$\mathcal{V} = \begin{pmatrix} -(\sigma_1+\mu)E_1 \\ -(\sigma_2+\mu)E_2 \\ p\sigma_1 E_1 - (\theta_1^a+\mu)I_1^a \\ (1-p)\sigma_1 E_1 - (\theta_1^s+\omega_1+\mu+\delta_1^s)I_1^s \\ q\sigma_2 E_2 - (\theta_2^a+\mu)I_2^a, \\ (1-q)\sigma_2 E_2 - (\theta_2^s+\omega_2+\mu+\mu_2^s)I_2^s \\ \omega_1 I_1^s + \omega_2 I_2^s - (\theta_1^h+\mu+\mu^h)H \end{pmatrix}. \quad (11)$$

The non-negative matrix F and the non-singular M-matrix V for the new infection terms and the remaining transfer terms are given by Eq. (12) in Box I and Eq. (13).

$$V = \begin{pmatrix} -g_1 & 0 & 0 & 0 & 0 & 0 & 0 \\ 0 & -g_2 & 0 & 0 & 0 & 0 & 0 \\ p\sigma_1 & 0 & -g_3 & 0 & 0 & 0 & 0 \\ (1-p)\sigma_1 & 0 & 0 & -g_4 & 0 & 0 & 0 \\ 0 & q\sigma_2 & 0 & 0 & -g_5 & 0 & 0 \\ 0 & (1-q)\sigma_2 & 0 & 0 & 0 & -g_6 & 0 \\ 0 & 0 & 0 & \omega_1 & 0 & \omega_2 & -g_7 \end{pmatrix}. \quad (13)$$

Thus, the effective reproduction number is given as in Box II, where

$N^0 = \dfrac{\Lambda}{\mu},\ g_1 = \sigma_1+\mu,\ g_2 = \sigma_2+\mu,\ g_3 = \theta_1^a+\mu,\ g_4 = \theta_1^s+\omega_1+\mu+\mu_1^s,$
$g_5 = \theta_2^a+\mu,\ g_6 = \theta_2^s+\omega_2+\mu+\mu_2^s,\ g_7 = \theta^h+\mu+\mu^h.$

Appendix B. Proof of Theorem 2

To prove that the DFE is GAS when $\mathcal{R}_c(v_1, v_2, v_3) < 1$, we have to verify the conditions $\mathcal{C}_1$ to $\mathcal{C}_3$.

Using [35], we obtain that the DFE $\mathcal{E}_0$ is LAS when $\mathcal{R}_c(v_1, v_2, v_3) < 1$, so the condition $\mathcal{C}_1$ is verified.

Next, we re-write system (1) in the form given in (6):

$$\frac{dX}{dt} = F(X,I) = \begin{pmatrix} \Lambda + \gamma R + u_1 V_1 + u_2 V_2 + u_3 V_3 - (\lambda_0+v_1+\mu)S \\ v_1 S - (\lambda_1+u_1+v_2+\mu)V_1 \\ v_2 V_1 - (\lambda_2+u_2+v_3+\mu)V_2 \\ v_3 V_2 - (\lambda_3+u_3+\mu)V_3 \\ \theta_1^a I_1^a + \theta_1^s I_1^s + \theta_2^a I_2^a + \theta_2^s I_2^s + \theta^h H - (\gamma+\mu)R \end{pmatrix}, \quad (15)$$

and

$$\frac{dI}{dt} = G(X,I) = \begin{pmatrix} \lambda_0 S + \lambda_1 V_1 - (\sigma_1+\mu)E_1 \\ \lambda_2 V_2 + \lambda_3 V_3 - (\sigma_2+\mu)E_2 \\ p\sigma_1 E_1 - (\theta_1^a+\mu)I_1^a \\ (1-p)\sigma_1 E_1 - (\theta_1^s+\omega_1+\mu+\mu_1^s)I_1^s \\ q\sigma_2 E_2 - (\theta_2^a+\mu)I_2^a \\ (1-q)\sigma_2 E_2 - (\theta_2^s+\omega_2+\mu+\mu_2^s)I_2^s \\ \omega_1 I_1^s + \omega_2 I_2^s - (\theta^h+\mu+\mu^h)H \end{pmatrix}. \quad (16)$$

We have

$$\frac{dX}{dt} = F(X_0, 0) \Leftrightarrow \begin{cases} \dot{S} = \Lambda + \gamma R + u_1 V_1 + u_2 V_2 + u_3 V_3 - (v_1+\mu)S, \\ \dot{V}_1 = v_1 S - (u_1+v_2+\mu)V_1, \\ \dot{V}_2 = v_2 V_1 - (u_2+v_3+\mu)V_2, \\ \dot{V}_2 = v_3 V_2 - (u_3+\mu)V_3, \\ \dot{R} = -(\gamma+\mu)R \end{cases}. \quad (17)$$

$$\mathcal{R}_c(v_1,v_2,v_3) = \frac{g_2g_5g_6\sigma_1(\beta S^0+\beta_1V_1^0)\left[g_4g_7p\xi_1+g_3(1-p)(g_7+\omega_1)\right]+g_1g_3g_4\sigma_2(\beta_2V_2^0+\beta_3V_3^0)\left[g_6g_7q\xi_2+g_5(1-q)(g_7+\omega_2)\right]}{g_1g_2g_3g_4g_5g_6g_7N^0}, \tag{14}$$

Box II.

$$\mathcal{A}=\mathcal{D}_Z\mathcal{G}(\mathcal{E}_0)=\begin{pmatrix} -g_1 & 0 & \xi_1\dfrac{\beta S^0+\beta_1V_1^0}{N^0} & \dfrac{\beta S^0+\beta_1V_1^0}{N^0} & \xi_2\dfrac{\beta S^0+\beta_1V_1^0}{N^0} & \dfrac{\beta S^0+\beta_1V_1^0}{N^0} & \dfrac{\beta S^0+\beta_1V_1^0}{N^0}\\ 0 & -g_2 & \xi_1\dfrac{\beta_2V_2^0+\beta_3V_3^0}{N^0} & \dfrac{\beta_2V_2^0+\beta_3V_3^0}{N^0} & \xi_2\dfrac{\beta_2V_2^0+\beta_3V_3^0}{N^0} & \dfrac{\beta_2V_2^0+\beta_3V_3^0}{N^0} & \dfrac{\beta_2V_2^0+\beta_3V_3^0}{N^0}\\ p\sigma_1 & 0 & -g_3 & 0 & 0 & 0 & 0\\ (1-p)\sigma_1 & 0 & 0 & -g_4 & 0 & 0 & 0\\ 0 & q\sigma_2 & 0 & 0 & -g_5 & 0 & 0\\ 0 & (1-q)\sigma_2 & 0 & 0 & 0 & -g_6 & 0\\ 0 & 0 & 0 & \omega_1 & 0 & \omega_2 & -g_7 \end{pmatrix}.$$

Box III.

This equation has a unique equilibrium point $\left(S^0, V_1^0, V_2^0, V_3^0, 0\right)$ (where S^0, V_1^0, V_2^0 and V_3^0 are given in (9)) which is globally asymptotically stable. Therefore, the condition $\mathcal{C}_2$ is satisfied.

Linearizing the matrix in Eq. (16) gives the Metzler Matrix in Box III. Computing $\hat{\mathcal{G}}(X,Z)$ with some algebraic simplification we obtain

$$\hat{\mathcal{G}}(X,I)=\mathcal{A}I-\mathcal{G}(X,I)$$
$$=\begin{pmatrix} (\xi_1I_1^a+I_1^s+\xi_2I_2^a+I_2^s+H)\left[\beta\left(\dfrac{S^0}{N_h^0}-\dfrac{S}{N_h}\right)+\beta_1\left(\dfrac{V_1^0}{N_h^0}-\dfrac{V_1}{N_h}\right)\right]\\ (\xi_1I_1^a+I_1^s+\xi_2I_2^a+I_2^s+H)\left[\beta_2\left(\dfrac{V_2^0}{N_h^0}-\dfrac{V_2}{N_h}\right)+\beta_3\left(\dfrac{V_3^0}{N_h^0}-\dfrac{V_3}{N_h}\right)\right]\\ 0\\0\\0\\0\\0 \end{pmatrix}$$

We have

$$\hat{\mathcal{G}}(X,I)\geq$$
$$\begin{pmatrix} (\xi_1I_1^a+I_1^s+\xi_2I_2^a+I_2^s+H)\left[\beta S^0\left(\dfrac{1}{N_h^0}-\dfrac{1}{N_h}\right)+\beta_1V_1^0\left(\dfrac{1}{N_h^0}-\dfrac{1}{N_h}\right)\right]\\ (\xi_1I_1^a+I_1^s+\xi_2I_2^a+I_2^s+H)\left[\beta_2V_2^0\left(\dfrac{1}{N_h^0}-\dfrac{1}{N_h}\right)+\beta_3V_3^0\left(\dfrac{1}{N_h^0}-\dfrac{1}{N_h}\right)\right]\\ 0\\0\\0\\0\\0 \end{pmatrix}$$

Knowing that $\left(\dfrac{1}{N_h^0}-\dfrac{1}{N_h}\right)=\dfrac{N_h-N_h^0}{N_hN_h^0}$ and that when $\mu_1^s=\mu_2^s=\mu^h=0$, $N_h(t)-N_h^0=\left(\dfrac{\Lambda}{\mu_h}-N_h(0)\right)(1-\exp(-\mu_ht))$ is positive, we obtain $\hat{\mathcal{G}}(X,I)\geq 0$. The condition $\mathcal{C}_3$ is satisfied. We can conclude that if $\mu_1^h=\mu_2^h=\mu^h=0$ then the DFE is GAS when $\mathcal{R}_c(v_1,v_2,v_3)<1$.

Appendix C. Proof of Theorem 3

Let $h_i=1-\epsilon_i$, $1\leq i\leq 3$, so $\lambda_i=h_i\lambda_0$.

After a few computations, we obtain the following expressions of each component of the endemic equilibrium depending on λ_0:

$$\begin{aligned}
V_1^\star &= \frac{v_1\Lambda}{G_1G_2+G_2\lambda_0^\star+(G_1\lambda_0^\star+\lambda_0^{2\star})h_1-u_1v_1},\\
S^\star &= \frac{h_1\lambda_0^\star+G_2}{v_1}V_1^\star,\\
V_2^\star &= \frac{h_2\lambda_0^\star+G_3}{v_2}V_1^\star,\\
V_3^\star &= \frac{h_3\lambda_0^\star+G_4}{v_3}V_2^\star,\\
E_1^\star &= \frac{\lambda_0^\star(S^\star+h_1V_1^\star)}{g_1},\\
E_2^\star &= \frac{\lambda_0^\star(h_2V_2^\star+h_3V_3^\star)}{g_2},\\
I_1^{a\star} &= \frac{p\sigma_1}{g_3}E_1^\star,\\
I_1^{s\star} &= \frac{(1-p)\sigma_1}{g_4}E_1^\star,\\
I_2^{a\star} &= \frac{q\sigma_2}{g_5}E_2^\star,\\
I_2^{s\star} &= \frac{(1-q)\sigma_2}{g_6}E_2^\star,\\
H^\star &= \frac{\omega_1I_1^{s\star}+\omega_2I_2^{s\star}}{g_7},\\
R^\star &= \frac{\theta_1^aI_1^{a\star}+\theta_1^sI_1^{s\star}+\theta_1^hH^\star+\theta_2^aI_2^{a\star}+\theta_2^sI_2^{s\star}}{G_5},\\
N^\star &= \frac{\Lambda-\mu_1^sI_1^{s\star}-\mu_2^sI_2^{s\star}-\mu^hH^\star}{\mu}.
\end{aligned} \tag{18}$$

By definition of the force of infection, we have $\lambda_0^\star=\beta\dfrac{I_1^{s\star}+I_2^{s\star}+H^\star+\xi_1I_1^{a\star}+\xi_2I_2^{a\star}}{N^\star}$.

When we replace $I_1^{s\star}$, $I_2^{s\star}$, $H^\star$ and $N^\star$ by their respective expressions, we obtain that $\lambda_0^\star$ is the solution of the following equation:

$$\lambda_0^\star\left(A_4\lambda_0^{\star4}+A_3\lambda_0^{\star3}+A_2\lambda_0^{\star2}+A_1\lambda_0^\star+A_0\right)=0, \tag{19}$$

Table C.3
Number of possible positive roots of Eq. (19) using Descartes's rule of signs.

Case	A_4	A_3	A_2	A_1	A_0	Possible positive roots	$\mathcal{R}_c$ condition
(i)	−	+	+	+	−	0 or 2	$\mathcal{R}_c < 1$
(ii)	−	+	+	+	+	1	$\mathcal{R}_c > 1$
(iii)	−	+	+	−	−	0 or 2	$\mathcal{R}_c < 1$
(iv)	−	+	+	−	+	1 or 3	$\mathcal{R}_c > 1$
(v)	−	+	−	+	−	0, 2 or 4	$\mathcal{R}_c < 1$
(vi)	−	+	−	+	+	1 or 3	$\mathcal{R}_c > 1$
(vii)	−	+	−	−	−	0 or 2	$\mathcal{R}_c < 1$
(viii)	−	+	−	−	+	1 or 3	$\mathcal{R}_c > 1$
(ix)	−	−	+	+	−	0 or 2	$\mathcal{R}_c < 1$
(x)	−	−	+	+	+	1	$\mathcal{R}_c > 1$
(xi)	−	−	+	−	−	0 or 2	$\mathcal{R}_c < 1$
(xii)	−	−	+	−	+	1 or 3	$\mathcal{R}_c > 1$
(xiii)	−	−	−	+	−	0 or 2	$\mathcal{R}_c < 1$
(xiv)	−	−	−	+	+	1	$\mathcal{R}_c > 1$
(xv)	−	−	−	−	−	0	$\mathcal{R}_c < 1$
(xvi)	−	−	−	−	+	1	$\mathcal{R}_c > 1$

where the coefficients

$$A_0 = (\mu(\mu + u_1 + v_1 + v_2) + v_1 v_2)(\mu + v_3) g_1 g_2 g_3 g_4 g_5 g_6 g_7 (\mathcal{R}_c - 1), \tag{20}$$

$$\begin{aligned} A_1 = {} & G_4 \beta g_2 g_4 g_5 g_6 g_7 h_1 h_2 \mu p \sigma_1 v_1 \xi_1 + G_3 \beta g_2 g_4 g_5 g_6 g_7 h_1 h_3 \mu p \sigma_1 v_1 \xi_1 \\ & + \beta g_1 g_3 g_4 g_6 g_7 h_2 h_3 \mu q \sigma_2 v_1 v_2 \xi_2 \\ & + G_4 \beta g_2 g_3 g_5 g_6 g_7 h_1 h_2 \mu p_1 \sigma_1 v_1 + G_3 \beta g_2 g_3 g_5 g_6 g_7 h_1 h_3 \mu p_1 \sigma_1 v_1 \\ & + G_4 \beta g_2 g_3 g_5 g_6 h_1 h_2 \mu \omega_1 p_1 \sigma_1 v_1 \\ & + G_3 \beta g_2 g_3 g_5 g_6 h_1 h_3 \mu \omega_1 p_1 \sigma_1 v_1 + \beta g_1 g_3 g_4 g_5 g_7 h_2 h_3 \mu q_1 \sigma_2 v_1 v_2 \\ & + \beta g_1 g_3 g_4 g_5 h_2 h_3 \mu \omega_2 q_1 \sigma_2 v_1 v_2 \\ & + G_3 G_4 \beta g_2 g_4 g_5 g_6 g_7 h_1 \mu p \sigma_1 \xi_1 + G_2 G_4 \beta g_2 g_4 g_5 g_6 g_7 h_2 \mu p \sigma_1 \xi_1 \\ & + G_2 G_3 \beta g_2 g_4 g_5 g_6 g_7 h_3 \mu p \sigma_1 \xi_1 \\ & + G_3 G_4 \beta g_2 g_3 g_5 g_6 g_7 h_1 \mu p_1 \sigma_1 + G_2 G_4 \beta g_2 g_3 g_5 g_6 g_7 h_2 \mu p_1 \sigma_1 \\ & + G_2 G_3 \beta g_2 g_3 g_5 g_6 g_7 h_3 \mu p_1 \sigma_1 \\ & + G_3 G_4 \beta g_2 g_3 g_5 g_6 h_1 \mu \omega_1 p_1 \sigma_1 + G_2 G_4 \beta g_2 g_3 g_5 g_6 h_2 \mu \omega_1 p_1 \sigma_1 \\ & + G_2 G_3 \beta g_2 g_3 g_5 g_6 h_3 \mu \omega_1 p_1 \sigma_1 \\ & + G_3 G_4 g_2 g_3 g_5 g_6 g_7 h_1 \mu_1 p_1 \sigma_1 v_1 + G_3 G_4 g_2 g_3 g_5 g_6 h_1 \mu_3 \omega_1 p_1 \sigma_1 v_1 \\ & + G_4 g_1 g_3 g_4 g_5 g_7 h_2 \mu_2 q_1 \sigma_2 v_1 v_2 \\ & + G_4 g_1 g_3 g_4 g_5 h_2 \mu_3 \omega_2 q_1 \sigma_2 v_1 v_2 + g_1 g_3 g_4 g_5 g_7 h_3 \mu_2 q_1 \sigma_2 v_1 v_2 v_3 \\ & + g_1 g_3 g_4 g_5 h_3 \mu_3 \omega_2 q_1 \sigma_2 v_1 v_2 v_3 \\ & - G_1 G_3 G_4 g_1 g_2 g_3 g_4 g_5 g_6 g_7 h_1 - G_1 G_2 G_4 g_1 g_2 g_3 g_4 g_5 g_6 g_7 h_2 \\ & - G_1 G_2 G_3 g_1 g_2 g_3 g_4 g_5 g_6 g_7 h_3 \\ & + G_2 G_3 G_4 g_2 g_3 g_5 g_6 g_7 \mu_1 p_1 \sigma_1 + G_2 G_3 G_4 g_2 g_3 g_5 g_6 \mu_3 \omega_1 p_1 \sigma_1 \\ & + G_4 g_1 g_2 g_3 g_4 g_5 g_6 g_7 h_2 u_1 v_1 \\ & + G_3 g_1 g_2 g_3 g_4 g_5 g_6 g_7 h_3 u_1 v_1 - G_2 G_3 G_4 g_1 g_2 g_3 g_4 g_5 g_6 g_7, \end{aligned} \tag{21}$$

$$\begin{aligned} A_2 = {} & \beta g_2 g_4 g_5 g_6 g_7 h_1 h_2 h_3 \mu p \sigma_1 v_1 \xi_1 + \beta g_2 g_3 g_5 g_6 g_7 h_1 h_2 h_3 \mu p_1 \sigma_1 v_1 \\ & + \beta g_2 g_3 g_5 g_6 h_1 h_2 h_3 \mu \omega_1 p_1 \sigma_1 v_1 \\ & + G_4 \beta g_2 g_4 g_5 g_6 g_7 h_1 h_2 \mu p \sigma_1 \xi_1 + G_3 \beta g_2 g_4 g_5 g_6 g_7 h_1 h_3 \mu p \sigma_1 \xi_1 \\ & + G_2 \beta g_2 g_4 g_5 g_6 g_7 h_2 h_3 \mu p \sigma_1 \xi_1 \\ & + G_4 \beta g_2 g_3 g_5 g_6 g_7 h_1 h_2 \mu p_1 \sigma_1 + G_3 \beta g_2 g_3 g_5 g_6 g_7 h_1 h_3 \mu p_1 \sigma_1 \\ & + G_2 \beta g_2 g_3 g_5 g_6 g_7 h_2 h_3 \mu p_1 \sigma_1 \\ & + G_4 \beta g_2 g_3 g_5 g_6 h_1 h_2 \mu \omega_1 p_1 \sigma_1 + G_3 \beta g_2 g_3 g_5 g_6 h_1 h_3 \mu \omega_1 p_1 \sigma_1 \\ & + G_2 \beta g_2 g_3 g_5 g_6 h_2 h_3 \mu \omega_1 p_1 \sigma_1 \\ & + G_4 g_2 g_3 g_5 g_6 g_7 h_1 h_2 \mu_1 p_1 \sigma_1 v_1 + G_3 g_2 g_3 g_5 g_6 g_7 h_1 h_3 \mu_1 p_1 \sigma_1 v_1 \\ & + G_4 g_2 g_3 g_5 g_6 h_1 h_2 \mu_3 \omega_1 p_1 \sigma_1 v_1 \\ & + G_3 g_2 g_3 g_5 g_6 h_1 h_3 \mu_3 \omega_1 p_1 \sigma_1 v_1 + g_1 g_3 g_4 g_5 g_7 h_2 h_3 \mu_2 q_1 \sigma_2 v_1 v_2 \\ & + g_1 g_3 g_4 g_5 h_2 h_3 \mu_3 \omega_2 q_1 \sigma_2 v_1 v_2 \\ & - G_1 G_4 g_1 g_2 g_3 g_4 g_5 g_6 g_7 h_1 h_2 - G_1 G_3 g_1 g_2 g_3 g_4 g_5 g_6 g_7 h_1 h_3 \\ & - G_1 G_2 g_1 g_2 g_3 g_4 g_5 g_6 g_7 h_2 h_3 \\ & + G_3 G_4 g_2 g_3 g_5 g_6 g_7 h_1 \mu_1 p_1 \sigma_1 + G_2 G_4 g_2 g_3 g_5 g_6 g_7 h_2 \mu_1 p_1 \sigma_1 \\ & + G_2 G_3 g_2 g_3 g_5 g_6 g_7 h_3 \mu_1 p_1 \sigma_1 \\ & + G_3 G_4 g_2 g_3 g_5 g_6 h_1 \mu_3 \omega_1 p_1 \sigma_1 + G_2 G_4 g_2 g_3 g_5 g_6 h_2 \mu_3 \omega_1 p_1 \sigma_1 \\ & + G_2 G_3 g_2 g_3 g_5 g_6 h_3 \mu_3 \omega_1 p_1 \sigma_1 \\ & + g_1 g_2 g_3 g_4 g_5 g_6 g_7 h_2 h_3 u_1 v_1 - G_3 G_4 g_1 g_2 g_3 g_4 g_5 g_6 g_7 h_1 \\ & - G_2 G_4 g_1 g_2 g_3 g_4 g_5 g_6 g_7 h_2 - G_2 G_3 g_1 g_2 g_3 g_4 g_5 g_6 g_7 h_3, \end{aligned} \tag{22}$$

$$\begin{aligned} A_3 = {} & \beta g_2 g_4 g_5 g_6 g_7 h_1 h_2 h_3 \mu p \sigma_1 \xi_1 + \beta g_2 g_3 g_5 g_6 g_7 h_1 h_2 h_3 \mu p_1 \sigma_1 \\ & + \beta g_2 g_3 g_5 g_6 h_1 h_2 h_3 \mu \omega_1 p_1 \sigma_1 + g_2 g_3 g_5 g_6 g_7 h_1 h_2 h_3 \mu_1 p_1 \sigma_1 v_1 \\ & + g_2 g_3 g_5 g_6 h_1 h_2 h_3 \mu_3 \omega_1 p_1 \sigma_1 v_1 - G_1 g_1 g_2 g_3 g_4 g_5 g_6 g_7 h_1 h_2 h_3 \\ & + G_4 g_2 g_3 g_5 g_6 g_7 h_1 h_2 \mu_1 p_1 \sigma_1 + G_3 g_2 g_3 g_5 g_6 g_7 h_1 h_3 \mu_1 p_1 \sigma_1 \\ & + G_2 g_2 g_3 g_5 g_6 g_7 h_2 h_3 \mu_1 p_1 \sigma_1 + G_4 g_2 g_3 g_5 g_6 h_1 h_2 \mu_3 \omega_1 p_1 \sigma_1 \\ & + G_3 g_2 g_3 g_5 g_6 h_1 h_3 \mu_3 \omega_1 p_1 \sigma_1 + G_2 g_2 g_3 g_5 g_6 h_2 h_3 \mu_3 \omega_1 p_1 \sigma_1 \\ & - G_4 g_1 g_2 g_3 g_4 g_5 g_6 g_7 h_1 h_2 - G_3 g_1 g_2 g_3 g_4 g_5 g_6 g_7 h_1 h_3 \\ & - G_2 g_1 g_2 g_3 g_4 g_5 g_6 g_7 h_2 h_3, \end{aligned} \tag{23}$$

$$\begin{aligned} A_4 = {} & -\mu(\mu + \mu_1^s + \omega_1)(\mu + \mu^h + \theta^h) - \mu(\mu + \mu^h + \omega_1) - \sigma_1 \theta^h (\mu + \omega_1 + p\mu_1^s) \\ & - \theta_1^s (\mu + \sigma_1)(\mu + \mu^h + \theta^h) - p\sigma_1(\mu_1^s(\mu + \mu^h) + \mu^h \omega_1). \end{aligned} \tag{24}$$

We then use Descartes's rule of signs to determine the existence of possible positive roots of Eq. (19). The results are summarized in Table C.3.

References

[1] https://covid19.who.int/.
[2] S. Lai, N. Ruktanonchai, L. Zhou, O. Prosper, W. Luo, J.R. Floyd, A. Wesolowski, M. Santillana, C. Zhang, X. Du, et al., Effect of non-pharmaceutical interventions to contain COVID-19 in China, Nature 585 (7825) (2020) 410–413.
[3] Y. Liu, C. Morgenstern, J. Kelly, R. Lowe, M. Jit, The impact of non-pharmaceutical interventions on SARS-CoV-2 transmission across 130 countries and territories, BMC Med. 19 (1) (2021) 1–12.
[4] K. Liu, Y. Lou, Optimizing COVID-19 vaccination programs during vaccine shortages: A review of mathematical models, Infect. Dis. Modell. (2022).
[5] O. Watson, G. Barnsley, J. Toor, A.B. Hogan, P. Winskill, A.C. Ghani, Global impact of the first year of COVID-19 vaccination: a mathematical modelling study, Lancet Infect. Dis. 22 (9) (2022) 1293–1302.
[6] A. Fontanet, S. Cauchemez, COVID-19 herd immunity: where are we? Nat. Rev. Immunol. 20 (10) (2020) 583–584.
[7] M. Jeyanathan, S. Afkhami, F. Smaill, M.S. Miller, B.D. Lichty, Z. Xing, Immunological considerations for COVID-19 vaccine strategies, Nat. Rev. Immunol. 20 (10) (2020) 615–632.
[8] https://covid19.trackvaccines.org/.
[9] P.S. Arunachalam, M.K. Scott, T. Hagan, C. Li, Y. Feng, F. Wimmers, L. Grigoryan, M. Trisal, V.V. Edara, L. Lai, et al., Systems vaccinology of the BNT162b2 mRNA vaccine in humans, Nature 596 (7872) (2021) 410–416.
[10] https://www.vidal.fr/actualites/27895-vaccins-contre-la-covid-19-la-troisieme-dose-pourquoi-pour-qui.html.

[11] B. Yang, Z. Yu, Y. Cai, The impact of vaccination on the spread of COVID-19: Studying by a mathematical model, Physica A 590 (2022) 126717.
[12] A. Olivares, E. Staffetti, Uncertainty quantification of a mathematical model of COVID-19 transmission dynamics with mass vaccination strategy, Chaos Solitons Fractals 146 (2021) 110895.
[13] P.C. Jentsch, M. Anand, C.T. Bauch, Prioritising COVID-19 vaccination in changing social and epidemiological landscapes: a mathematical modelling study, Lancet Infect. Dis. 21 (8) (2021) 1097–1106.
[14] M. Yavuz, F. Coşar, F.N. Özdemir, A new mathematical modeling of the COVID-19 pandemic including the vaccination campaign, Open J. Model. Simul. 9 (3) (2021) 299–321.
[15] Y. Choi, J.S. Kim, J.E. Kim, H. Choi, C.H. Lee, Vaccination prioritization strategies for COVID-19 in Korea: a mathematical modeling approach, Int. J. Environ. Res. Public Health 18 (8) (2021) 4240.
[16] D. Aldila, B. Samiadji, G.M. Simorangkir, S.H. Khosnaw, M. Shahzad, Impact of early detection and vaccination strategy in COVID-19 eradication program in Jakarta, Indonesia, BMC Res. Notes 14 (1) (2021) 1–7.
[17] A.D. Algarni, A.B. Hamed, M. Hamdi, H. Elmannai, S. Meshoul, Mathematical COVID-19 model with vaccination: a case study in Saudi Arabia, PeerJ Comput. Sci. 8 (2022) e959.
[18] A.K. Paul, M.A. Kuddus, Mathematical analysis of a COVID-19 model with double dose vaccination in Bangladesh, Results Phys. 35 (2022) 105392.
[19] F. Parino, L. Zino, G.C. Calafiore, A. Rizzo, A model predictive control approach to optimally devise a two-dose vaccination rollout: A case study on COVID-19 in Italy, Internat. J. Robust Nonlinear Control (2021).
[20] Y. Liu, C.A. Pearson, F.G. Sandmann, R.C. Barnard, J. Kim, S. Flasche, M. Jit, K. Abbas, C.C.-.W. Group, et al., Dosing interval strategies for two-dose COVID-19 vaccination in 13 middle-income countries of Europe: Health impact modelling and benefit-risk analysis, Lancet Reg. Health-Eur. (2022) 100381.
[21] P. Scarabaggio, R. Carli, G. Cavone, N. Epicoco, M. Dotoli, Modeling, estimation, and optimal control of anti-covid-19 multi-dose vaccine administration, in: 2021 IEEE 17th International Conference on Automation Science and Engineering, CASE, IEEE, 2021, pp. 990–995.
[22] H. Reyes, B. Diethelm-Varela, C. Méndez, D. Rebolledo-Zelada, B. Lillo-Dapremont, S.R. Muñoz, S.M. Bueno, P.A. González, A.M. Kalergis, Contribution of two-dose vaccination toward the reduction of COVID-19 cases, icu hospitalizations and deaths in chile assessed through explanatory generalized additive models for location, scale, and shape, Front. Public Health 10 (2022) 815036.
[23] X. Wang, H. Wang, P. Ramazi, K. Nah, M. Lewis, From policy to prediction: Forecasting COVID-19 dynamics under imperfect vaccination, Bull. Math. Biol. 84 (9) (2022) 90.
[24] S. Tchoumi, H. Rwezaura, J. Tchuenche, A mathematical model with numerical simulations for malaria transmission dynamics with differential susceptibility and partial immunity, Healthc. Anal. 3 (2023) 100165.
[25] M. Diagne, H. Rwezaura, S. Tchoumi, J. Tchuenche, A mathematical model of COVID-19 with vaccination and treatment, Comput. Math. Methods Med. 2021 (2021).
[26] E.A. Iboi, C.N. Ngonghala, A.B. Gumel, Will an imperfect vaccine curtail the COVID-19 pandemic in the US? Infect. Dis. Modell. 5 (2020) 510–524.
[27] A.F. Read, S.J. Baigent, C. Powers, L.B. Kgosana, L. Blackwell, L.P. Smith, D.A. Kennedy, S.W. Walkden-Brown, V.K. Nair, Imperfect vaccination can enhance the transmission of highly virulent pathogens, PLoS Biol. 13 (7) (2015) e1002198.
[28] F. Sulayman, F.A. Abdullah, M.H. Mohd, An SVEIRE model of tuberculosis to assess the effect of an imperfect vaccine and other exogenous factors, Mathematics 9 (4) (2021) 327.
[29] J.J. Bull, R. Antia, Which 'imperfect vaccines' encourage the evolution of higher virulence? Evol. Med. Public Health 10 (1) (2022) 202–213.
[30] L. Pezzoli, A.S. Azman, Moving forward with an imperfect vaccine, Lancet Infect. Dis. 21 (10) (2021) 1339–1341.
[31] H.L. Nyandjo Bamen, J.M. Ntaganda, A. Tellier, O. Menoukeu Pamen, Impact of imperfect vaccine, vaccine trade-off and population turnover on infectious disease dynamics, Mathematics 11 (5) (2023) 1240.
[32] T.S. Faniran, A. Ali, N.E. Al-Hazmi, J.K.K. Asamoah, T.A. Nofal, M.O. Adewole, New variant of SARS-CoV-2 dynamics with imperfect vaccine.
[33] A.B. Gumel, C.C. McCluskey, J. Watmough, An SVEIR model for assessing potential impact of an imperfect anti-SARS vaccine, 2006.
[34] Y. Yang, J. Li, Z. Ma, L. Liu, Global stability of two models with incomplete treatment for tuberculosis, Chaos Solitons Fractals 43 (1–12) (2010) 79–85.
[35] P. Van den Driessche, J. Watmough, Reproduction numbers and sub-threshold endemic equilibria for compartmental models of disease transmission, Math. Biosci. 180 (1–2) (2002) 29–48.
[36] O. Diekmann, J.A.P. Heesterbeek, J. Metz, On the definition and the computation of the basic reproduction ratio r 0 in models for infectious diseases in heterogeneous populations, J. Math. Biol. 28 (4) (1990) 365–382.
[37] C. Castillo-Chavez, Z. Feng, W. Huang, et al., On the computation of ro and its role on, in: Mathematical Approaches for Emerging and Reemerging Infectious Diseases: an Introduction, Vol. 1, 2002, p. 229.
[38] https://www.alberta.ca/stats/covid-19-alberta-statistics.htmldata-export.
[39] S. Pedro, H. Rwezaura, J. Tchuenche, Time-varying sensitivity analysis of an influenza model with interventions, Int. J. Biomath. 15 (03) (2022) 2150098.
[40] S. Tchoumi, H. Rwezaura, J. Tchuenche, Dynamic of a two-strain COVID-19 model with vaccination, Results Phys. 39 (2022) 105777.